
Article:
Bain, Calum C, Oliphant, Christopher J, Thomson, Carolyn A et al. (2 more authors) (2018) Pro-inflammatory role of monocyte-derived CX3CR1int macrophages in Helicobacter hepaticus-induced colitis. Infection and Immunity. e00579-17. ISSN 1098-5522

https://doi.org/10.1128/IAI.00579-17

Pro-inflammatory role of monocyte-derived CX3CR1^{int} macrophages in *Helicobacter hepaticus*-induced colitis

Calum C. Bain[1,3#], Christopher J. Oliphant[2,4], Carolyn A. Thomson[1], Marika C. Kullberg[2#] and Allan McI. Mowat[1]

[1]Centre for Immunobiology, Institute of Infection, Immunity and Inflammation, University of Glasgow, UK

[2]Centre for Immunology and Infection, Department of Biology and Hull York Medical School, University of York, UK

[3]Present address: MRC Centre for Inflammation Research, University of Edinburgh, UK

[4]Present address: Biosceptre Ltd, Cambridge, UK.

[#] Corresponding authors: Marika C. Kullberg and Calum C. Bain

Running title: Myeloid cells in *H. hepaticus* colitis

ABSTRACT

Cells of the monocyte-macrophage lineage play important roles in the pathogenesis of inflammatory bowel diseases, but they are also present in the normal healthy intestine, where they are critical for maintaining homeostasis. It has been unclear whether the pro-inflammatory roles of intestinal macrophages reflect altered behaviour of the existing resident cells, or if they involve recruitment of a distinct cell type. Here we have explored these ideas using the model of colitis induced by *Helicobacter hepaticus* (*Hh*) in the context of neutralisation or deletion of interleukin 10 (IL-10). Granulocytes and monocytes made up most of the inflammatory myeloid infiltrates found in the colon of *Hh*-infected colitic mice, rising to a peak within 2 weeks of *Hh* inoculation, but taking several months to resolve completely. The inflammatory response was dependent on the combined presence of *Hh* and absence of IL-10, and was accompanied by increased production of inflammatory mediators such as IL-1β, TNFα, IL-6 and IL-23p19 by infiltrating myeloid cells, mostly relatively immature cells of the macrophage lineage that express intermediate levels of CX3CR1. In contrast, the population of mature CX3CR1^{hi} macrophages did not expand as markedly during colitis, and these cells made little contribution to inflammatory mediator production. Taking into account their numerical dominance in the myeloid compartment, we conclude that newly recruited monocytes are the main source of pro-inflammatory mediators in colitis induced in the absence of IL-10 signalling, and that altered behaviour of mature macrophages is not a major component of this pathology.

INTRODUCTION

Inflammatory bowel diseases (IBD), comprising Crohn's disease and ulcerative colitis, are growing health problems in the developed world. Although recent advances have helped elucidate some of the mechanisms underlying IBD, treatment remains unsatisfactory and individual regimes are seldom effective for all patients. Thus, a better understanding of the processes and cells involved in the pathogenesis of IBD could help develop new targets for therapy.

Macrophages (mø) have received considerable attention in recent years because of their potential roles in both steady-state and inflamed intestine (1-3). Resident møs are abundant in the healthy intestine, where they are involved in clearance of apoptotic cells and play a crucial role in maintaining homeostasis, ingesting and killing commensal bacteria that cross the epithelial barrier (reviewed in (2)). In contrast to other tissues, these processes do not provoke overt inflammation in the intestine, due to powerful control mechanisms that prevent local mø from producing pro-inflammatory mediators in response to stimuli such as TLR ligands (4, 5). However, findings from both IBD and experimental models of the disease have demonstrated that møs are also crucial components of the inflammatory infiltrate (4, 6-9), raising the possibility of exploiting them as therapeutic targets.

We and others have shown recently that intestinal mø originate from Ly6C^{hi} blood monocytes that continuously enter the colonic mucosa and differentiate locally through a series of intermediaries. Although only present in small numbers, cells with the phenotypic and morphological features of Ly6C^{hi} monocytes can be found in the steady state mucosa. However, major transcriptional differences exist between these and Ly6C^{hi} monocytes found in blood, suggesting that the differentiation process occurs immediately after monocytes enter the colonic mucosa (6, 10). Importantly, as monocytes mature they progressively acquire anti-

inflammatory properties, such as constitutive production of IL-10 and hyporesponsiveness to e.g. TLR ligands (6, 11, 12). However, this physiological process is disrupted during inflammation (6, 12, 13), and understanding of how this change in mø behaviour occurs would be an important advance in our knowledge of how to prevent and treat IBD. Studies of the colitis induced by feeding dextran sodium sulphate (DSS) suggest that the tissue pathology is paralleled by the accumulation of highly pro-inflammatory monocytes, whereas the fully differentiated møs that remain do not alter their behaviour and retain their anti-inflammatory characteristics (6, 12). However, it is not clear if this pattern extends to other forms of intestinal inflammation, particularly under conditions where there are intrinsic defects in the mechanisms that normally control resident mø function.

The IL-10 – IL-10R axis is an important brake on mø activation, particularly in the intestine, where deletion of either the cytokine or its receptor leads to spontaneous onset of inflammation in association with hyper-responsiveness of mø (13-19). Furthermore, humans with non-functional mutations in *IL10*, *IL10RA*, or *IL10RB* develop severe enterocolitis within the first months of life (reviewed in (20)). Here we have examined the relationship between IL-10 and the differentiation of intestinal mø in inflammation in more depth by exploring mø behaviour during colitis induced by inoculation of mice with *Helicobacter hepaticus* (*Hh*) in the absence of IL-10 signalling (21, 22). We report that *Hh*-induced colitis is characterized by the accumulation of pro-inflammatory $CD11b^{+}$ myeloid cells that are hyper-responsive to TLR stimulation. Most of these cells are monocytes and their immediate progeny that express intermediate levels of CX3CR1 and that have not differentiated fully into anti-inflammatory, resident-type $CX3CR1^{hi}$ mø. We further show that the expansion of cells in the monocyte-mø compartment is maintained for several months before returning to normal levels as the inflammation resolves.

MATERIALS AND METHODS

Infection and antibody treatment of mice

Female C57BL/6 (B6) *Il10*$^{-/-}$, B6 WT, B6 CD45.1^{+} *Cx3cr1*$^{gfp/gfp}$ mice (obtained from Jackson Laboratory), and B6 CD45.1^{+} *Cx3cr1*$^{+/gfp}$ (generated by crossing *Cx3cr1*$^{gfp/gfp}$ mice with B6 CD45.1^{+} WT animals) were bred and maintained in an accredited SPF facility, and the experiments were conducted in accordance with the UK Animals (Scientific Procedures) Act 1986 under a Project License authorized by the UK Home Office and approved by the University of York Animal Welfare and Ethical Review Body. The mice tested negative for antibodies to specific murine viruses, were free of *Helicobacter spp.* as assessed by PCR, and were >6-weeks old when used.

Mice were allocated to treatment groups and inoculated i.g. with 1.5 x 10^7 *Hh* NCI-Frederick isolate 1A (23), derived originally from the same mouse colony as isolate Hh-1 (24) (American Type Culture Collection strain 51449). IL-10-sufficient mice were also treated i.p. with 1 mg of anti-IL-10R (clone 1B1.3a) on days 0, 7, 14, 21, 28, 35, 42, 49, 56, 63, and 70 of *Hh* infection. Age- and sex-matched uninfected animals were included as controls. One week after the last mAb injection, mice were sacrificed and intestines collected for analysis.

Lamina propria (LP) cell isolation

For the experiments shown in Figures 1 and 2, colon and caecum were pooled from individual mice and digested with Liberase CI (0.42 mg/ml, Roche, Burgess Hill, UK) and DNase I (125 U/ml; Sigma-Aldrich, Gillingham, UK), followed by enrichment of LP cells on 40/80% Percoll gradients as described previously (25). For the experiments shown in Figures 3-5 and in Supplementary Figures, colonic LP cells were isolated as described previously without the use of Percoll gradients (4, 26).

115

116 **Flow cytometric analysis and FACS**

117 After blocking Fc receptors with anti-FcγRII/III mAb (2.4G2; BD Biosciences), LP cells were
118 stained at 4°C with fluorochrome-conjugated antibodies (see Table S1) for 20-30 min in the
119 dark before being washed in FACS buffer (2% FCS and 1mM EDTA in PBS) and then
120 analyzed on a CyAn ADP (Beckman Coulter, High Wycombe, UK) or LSRII/FACSAria I (BD
121 Bioscience) flow cytometer. Data were analyzed using FlowJo software (Tree Star Inc. OR,
122 USA). Myeloid cell populations (as defined in figure legends) were sorted using a MoFlo
123 Astrios or a FACSAria I sorter, with purities of >96%. For flow cytometric analyses on BD
124 instruments, automatic compensation was performed in FACSDiva using UltraComp or
125 OneComp beads together with fluorescence minus one controls.

126

127 **Intracellular cytokine staining (ICS)**

128 Large intestinal LP cells (2 x 10^6/ml) from uninfected and 2-week *Hh*-infected *Il10*$^{-/-}$ mice
129 were cultured in medium alone or in the presence of 10 μg/ml Pam3CSK4 (Invivogen,
130 Toulouse, France) for 4 hr at 37°C with 10 μg/ml brefeldin A during the last 3 hr. Thereafter,
131 cells were stained for surface markers (CD45 and CD11b) and intracellular TNF-α as
132 described previously (25).

133

134 **Analysis of cytokine protein and mRNA expression**

135 For cytokine protein analysis, FACS-purified CD45$^+$CD11b$^+$ cells were cultured in 96-well
136 round-bottomed plates (5x10^4/ml; 0.2ml/well) at 37°C and 5% CO_2 in medium alone or with 10
137 μg/ml ultrapure *E. coli* LPS, 10 μg/ml Pam3CSK4 (both from Invivogen, Toulouse, France) or
138 10 μg/ml soluble *Hh* antigen (SHelAg) prepared as described (21, 27). After 24 hr,

supernatants were collected and analyzed by ELISA for IL-12p40 (Mabtech, Nacka Strand, Sweden) and IL-6 (R&D Systems), and by FlowCytomix for TNF-α (Bender MedSystems, Vienna, Austria).

For cytokine RT-qPCR analysis in Fig. 2, FACS-purified $CD45^+CD11b^+$ cells were homogenized in TRIzol, and total RNA isolated by chloroform extraction and reverse transcribed using SuperScript II and random hexamers. cDNA was amplified using SYBR green reagents and an ABI Prism RT-PCR system (Applied Biosystems). Cytokine expression levels for each individual sample (run in duplicates) were normalized to HPRT using ΔCt calculations and the 7000 system SDS software (Applied Biosystems). For myeloid cell populations in Fig. 5, FACS-purified cells were lysed in RLT buffer (Qiagen) and homogenised using Qiashredders (Qiagen). RNA was then isolated and purified using an RNeasy micro kit (Qiagen) and reverse transcribed using a High Capacity RNA-to-cDNA kit (Life Technologies) and random hexamers. cDNA was amplified using SYBR green reagents and an ABI 7900HT Prism RT-PCR system (Applied Biosystems). Cytokine expression levels for each individual sample (run in triplicates) were normalized to TBP using ΔCt calculations. Specific primers pairs are detailed in Table S2.

Statistical analysis

Multiple group comparisons were performed by one-way ANOVA, while Student's t-test and Mann Whitney test was used to compare two groups. Differences were considered statistically significant with $P<0.05$.

RESULTS

Expansion of myeloid cells in the large intestine of *Hh*-infected colitic *Il10*$^{-/-}$ mice.

To begin to characterize the innate immune response in the large intestine following *Hh* inoculation, WT and *Il10*$^{-/-}$ mice were inoculated i.g. with the bacterium, and the cellular composition of LP cells from pooled ceca and colons was examined 2 weeks later, the time point at which pathology peaks in *Il10*$^{-/-}$ hosts (25). As expected, *Hh*-infected *Il10*$^{-/-}$ mice displayed enhanced cellularity of the large intestinal LP compared with uninfected controls (Fig. 1A, left panel), with greatly expanded proportions and numbers of CD45^{+} hematopoietic cells (Fig. 1A, middle and right panels), consisting of B cells, CD4^{+} T cells, and CD11b^{+} myeloid cells (Fig. 1B). Only minor increases were observed in the proportion and number of LP CD45^{+} cells in *Hh*-infected WT mice (Fig. 1A), and the size of CD11b^{+} myeloid compartment was unaffected in these hosts (Fig. 1B, right panel). More detailed analysis of the early cellular kinetics following *Hh* inoculation of *Il10*$^{-/-}$ animals revealed that the numbers of total CD45^{+} cells and of CD11b^{+} myeloid cells were significantly increased in *Hh*-infected *Il10*$^{-/-}$ mice on day 5 pi, and expanded steadily until day 11 pi (Fig. 1C). Thus, *Hh*-driven typhlocolitis in *Il10*$^{-/-}$ mice is associated with massive infiltration by both lymphoid and myeloid cells.

Myeloid cells from *Hh-infected Il10*$^{-/-}$ mice display a pro-inflammatory phenotype

To understand how the expansion of the myeloid compartment might contribute to the colitis in *Il10*$^{-/-}$ hosts, we examined the cytokine secretion profile of CD11b^{+} cells from uninfected and *Hh*-infected *Il10*$^{-/-}$ mice. To this end, large intestinal LP cells were stimulated with the TLR ligand Pam3CSK4, and TNFα production examined by intracellular cytokine staining (ICS). TLR ligation of LP cells from *Hh*-infected *Il10*$^{-/-}$ animals resulted in ~3-fold increase in

the proportion of CD11b$^+$ cells producing TNFα compared with cells cultured in medium alone (Fig. 2A, bottom panels), and this translated to a highly significant increase in the absolute number of TNFα^+CD11b$^+$ cells in the LP of infected *Il10*$^{-/-}$ mice compared with uninfected controls (Fig. 2B). In contrast, the proportion of TNFα^+ CD11b$^+$ cells from uninfected *Il10*$^{-/-}$ animals was unaffected by Pam3CSK4 stimulation and remained at levels similar to those seen in naïve WT colon (Fig. 2A, upper panels and Fig. 2B).

To extend these analyses, we next FACS-purified CD11b$^+$ cells from the large intestinal LP of uninfected and 2-week *Hh*-infected *Il10*$^{-/-}$ animals and cultured them overnight with LPS, Pam3CSK4, or soluble *Hh* antigen (SHelAg), before assessing the levels of a wider range of cytokines using ELISA and FlowCytoMix. CD11b$^+$ cells from *Hh*-infected *Il10*$^{-/-}$ mice secreted higher amounts of IL-12p40, IL-6, and TNFα after all forms of stimulation compared with CD11b$^+$ cells from uninfected *Il10*$^{-/-}$ hosts (Fig. 2C). When analysed directly *ex vivo*, FACS-purified CD11b$^+$ cells from *Hh*-infected *Il10*$^{-/-}$ mice also contained higher levels of *Il12a* and *Il23a* transcripts compared with CD11b$^+$ cells from uninfected controls, whereas the levels of *Il12b* accumulation were similar in the two populations (Fig. 2D). Thus, the expanded myeloid cell compartment in the large intestine of *Hh*-infected colitic *Il10*$^{-/-}$ mice displays pro-inflammatory characteristics.

Composition of the myeloid compartment in *Hh*-infected *Il10*$^{-/-}$ mice

We next set out to explore what cell types accounted for the change within the CD11b$^+$ compartment during *Hh* colitis. To do this, we exploited multiparameter flow cytometry and rigorous gating strategies we have developed recently to characterise the myeloid compartment of the intestinal LP, allowing precise identification of monocytes, mø, eosinophils, neutrophils and dendritic cells (DC) ((6); Fig. S1). We also omitted the Percoll

gradient step during the purification to exclude the possibility of selective loss of individual cell types. These approaches confirmed marked changes in the composition of the myeloid cell compartment in the colon 2 weeks after *Hh* inoculation of *Il10*$^{-/-}$ mice, compared with uninfected *Il10*$^{-/-}$ mice or *Hh*-infected WT mice (Fig. 3A). Ly6G^{+} neutrophils and SSC^{hi} (MHCII^{-}) eosinophils (Figs. 3A, B and C) accounted for a substantial part of the infiltration found in *Hh*-infected *Il10*$^{-/-}$ mice and no significant differences were seen in these granulocyte populations in *Hh*-infected WT mice, or in uninfected *Il10*$^{-/-}$ mice compared with uninfected WT mice (Figs. 3A, B, and C).

Hh-infected *Il10*$^{-/-}$ mice also showed marked expansion in the numbers of non-granulocytic myeloid cells (Figs. 3A, D and E), and we therefore explored the contribution of monocytes and mø in more detail. To do this, we focused on cells expressing the pan-mø markers F4/80 and/or CD64 (Fig. S1) and examined the monocyte-mø differentiation continuum that we and others have defined in the colonic LP (6, 28, 29). This so-called 'monocyte waterfall' consists of newly arrived Ly6C^{hi}MHCII^{-} monocytes, differentiating Ly6C^{+}MHCII^{+} monocytes, and more mature Ly6C^{-}MHCII^{+} cells that include tissue-resident mø (Fig. 3D). *Hh*-infected *Il10*$^{-/-}$ mice showed marked increases in the proportions and absolute numbers of Ly6C^{hi}MHCII^{-} and Ly6C^{+}MHCII^{+} cells, which were increased by ~125-fold and 155-fold respectively compared with their numbers in uninfected *Il10*$^{-/-}$ mice (Figs. 3D and E). There was also a modest, but significant increase in the number of more mature Ly6C^{-} MHCII^{+} cells in *Hh*-infected *Il10*$^{-/-}$ mice (Fig. 3E, right panel). *Hh*-infected WT mice, which do not develop colitis, showed some evidence of increased infiltration by Ly6C^{hi}MHCII^{-}, Ly6C^{+}MHCII^{+} and Ly6C^{-} cells, while uninfected *Il10*$^{-/-}$ mice had slightly higher numbers of Ly6C^{+}MHCII^{+} cells compared with their naïve WT counterparts; however, these differences were modest and did not attain statistical significance (Fig. 3E).

DCs were identified as $CD11c^{+}MHCII^{+}CD64^{-}$ cells amongst LP leukocytes (30) and their numbers increased in *Hh*-infected compared to control *Il10*$^{-/-}$ mice (Fig. S2A). The frequency of DCs among LP cells of *Hh*-infected *Il10*$^{-/-}$ mice decreased compared to uninfected controls (data not shown), most likely reflecting the increase in other leukocytes. Finally, there were minor changes in the proportion of DC subsets identified on the basis of CD11b and CD103 expression, although none of these changes reached statistical significance (Fig. S2B).

Altered monocyte - mø differentiation in *Hh*-infected colitic mice

The accumulation of monocytes we found in *Hh* colitis is reminiscent of our own and other results from DSS and T-cell-mediated colitis, where there appeared to be an arrest in the local differentiation continuum that normally generates anti-inflammatory, resident mø (6, 12, 28). To examine whether a similar block was present during *Hh*-induced colitis, we used *Cx3cr1*$^{+/gfp}$ reporter mice in which one allele of the *Cx3cr1* gene has been replaced with the gene encoding green fluorescent protein (GFP) (31). This allows fully differentiated resident $CX3CR1^{hi}$ mø to be distinguished from cells in the earlier $CX3CR1^{int}$ stages in the developmental continuum, some of which would have been included amongst the $Ly6C^{-}$ $MHCII^{+}$ population we defined earlier. In this way, we could examine the relative roles of resident and recently recruited mø in *Hh*-induced inflammation, as well as explore how these cells behave during the resolution of pathology that occurs at later stages after bacterial inoculation (25). Because the *Cx3cr1*$^{+/gfp}$ reporter mice are IL-10 sufficient, we had to induce colitis by *Hh* inoculation plus weekly administration of anti-IL-10R mAb (22). Consistent with our studies in *Il10*$^{-/-}$ mice, this resulted in massive accumulation of total leukocytes and $CD11b^{+}$ myeloid cells in the colonic mucosa by day 14 pi (Figs. 4A and B). However, by day

41 pi, both compartments had contracted significantly, and by day 77 pi they were both reduced almost to baseline levels (Figs. 4A and B).

As in colitic *Il10*$^{-/-}$ mice, the composition of the myeloid compartment was markedly altered in anti-IL-10R-treated *Hh*-infected *Cx3cr1*$^{+/gfp}$ mice, with a large expansion of granulocytes and monocyte-derived cells at day 14 pi, followed by resolution at later times (Fig. 4C). Moreover, the non-granulocyte component of the myeloid infiltrate contained large numbers of Ly6C^{hi}MHCII^{-} and Ly6C^{+}MHCII^{+} cells at day 14 pi (Figs. 4C-E). The Ly6C^{-}MHCII^{+} population also expanded in number early in colitis, but most of this expansion was accounted for by CX3CR1^{int} cells (Fig. 4F), a population that we have shown previously to be a further intermediary stage in the local differentiation of monocytes (6). In parallel, there was a substantial decrease in the proportion of fully-mature CX3CR1^{hi} mø amongst the Ly6C^{-} MHCII^{+} cells at this time (Fig. 4F), although their absolute numbers were increased and remained so throughout the experiment (Fig. 4G). By day 41 pi, the proportions and numbers of CX3CR1^{int} cells amongst Ly6C^{-}MHCII^{+} cells had contracted significantly, and by day 77 pi, CX3CR1^{hi} cells had again come to dominate the Ly6C^{-} mature mø compartment (Fig. 4F & G). At this time the numbers of Ly6C^{hi}MHCII^{-} and Ly6C^{+}MHCII^{+} cells had also returned to baseline levels (Fig. 4E).

The numbers of Ly6G^{+} neutrophils and CD11c^{+}CD11b^{+}F4/80^{-} DC were greatly increased by day 14 pi in anti-IL-10R-treated *Hh*-infected *Cx3cr1*$^{+/gfp}$ mice, before falling at later times in parallel with the reduction in monocytes and mø (Fig. S3A and B). Interestingly however, the numbers of colonic eosinophils remained high in these mice until the end of the experiment on day 77 pi (Fig. S3C). All these *Hh*-induced changes in myeloid cells were seen only when *Hh*-infected *Cx3cr1*$^{+/gfp}$ mice were also co-administered with anti-IL-10R (Fig. 4 and data not shown). Anti-IL-10R treatment alone of uninfected *Cx3cr1*$^{+/gfp}$ mice did not result in

leukocyte accumulation in the colonic mucosa (Fig. S4), findings that are in agreement with those we previously reported for uninfected WT mice (22).

Together our results demonstrate that the acute phase of *Hh*-induced colitis is associated with accumulation of CX3CR1^{int} monocytes and early-stage mø, consistent with the idea that there may be a block in the normal differentiation process.

Colonic CX3CR1^{int} monocytes/møs are the major producers of pro-inflammatory cytokines during *Hh* colitis

Finally we explored whether elicited CX3CR1^{int} cells were responsible for the production of pro-inflammatory mediators by myeloid cells during colitis, or if this reflected altered behaviour of the more mature CX3CR1^{hi} mø. RT-qPCR analysis showed marked upregulation of mRNA transcripts for *Il1b*, *Nos2* (iNOS), *Il23p19* and *Il12p35* in CX3CR1^{int} cells from anti-IL-10R-treated *Hh*-infected mice at the peak of inflammation on day 14 compared with CX3CR1^{int} cells from control mice (Fig. 5A-D). In contrast, colonic CX3CR1^{hi} mø from anti-IL-10R-treated *Hh*-infected mice showed only minor changes in mRNA levels of pro-inflammatory mediators (Fig. 5). Thus, taking into account their numerical dominance in the myeloid compartment, newly recruited CX3CR1^{int} monocytes/møs form the predominant pro-inflammatory population in this model of colitis.

DISCUSSION

The results presented here underline the importance of the myeloid compartment in the inflammatory colitis that occurs in mice infected with *Helicobacter hepaticus* when IL-10-mediated signalling is absent. Using a variety of approaches to identify myeloid lineages,

305 including *Cx3cr1*$^{+/gfp}$ mice, we show that an intense infiltrate of CD11b^{+} cells appears early
306 during infection and that this is made up of neutrophils, eosinophils, Ly6C^{hi}MHC$^{-/+}$ monocytes
307 and CX3CR1^{int} mϕ at the time of peak disease at 2 weeks after *Hh* inoculation. While this
308 confirms other work (32), we also show here that this expansion of the monocyte-mϕ
309 compartment is sustained for up to 11 weeks after infection, by which time other parameters
310 of inflammation, such as changes in myeloid cell subset composition, have returned to
311 steady-state levels. Importantly, the inflammatory changes required both infection with *Hh* and
312 neutralisation of IL-10R signalling, with very few changes being seen in mice with *Hh* infection
313 alone or loss of IL-10 alone. Similarly, the greatly heightened production of pro-inflammatory
314 mediators in response to activation *in vitro* by intestinal myeloid cells was fully dependent on
315 these factors operating together. These results confirm previous conclusions that *Hh* plays a
316 crucial role in provoking intestinal inflammation in the absence of IL-10-mediated
317 immunoregulation and that pro-inflammatory responses to this organism are normally
318 restrained by IL-10 (21, 22, 33).

319 In previous work, we have shown that resident mϕ in normal intestinal mucosa are
320 replenished continuously by Ly6C^{hi} monocytes that differentiate via a number of intermediary
321 stages into mature, resident mϕ (6, 11, 28). At early times after inoculation with *Hh*, this so-
322 called monocyte-mϕ "waterfall" expanded dramatically, and consisted mostly of Ly6C^{hi}MHCII^{-}
323 $^{/+}$ monocytes and CX3CR1^{int} mϕ, with less expansion of fully mature CX3CR1^{hi} mϕ. Although
324 these findings are consistent with previous work, e.g. in chemically-induced colitis (6), and
325 suggest that the normal process of monocyte-mϕ differentiation is arrested, it is important to
326 note that the absolute numbers of mature mϕ were actually increased in our mice with *Hh*-
327 induced colitis and remained so for the duration of the 11-week experiment. Thus, although
328 the majority of infiltrating monocytes may be short-lived in the colitic mucosa, a proportion of

these cells may still develop into mature CX3CR1^{hi} mϕ, even in the face of inflammation. How the mϕ recruited under these conditions might contribute to the inflammation or its resolution and if they eventually acquire all the properties of the normal, resident population remain to be determined, as do the relative contributions of newly recruited and pre-existing cells to the "resident" mϕ compartment.

Although methods were not available to examine and track infiltrating monocytes directly following their arrival in the gut, we were able to explore whether the total mature mϕ population was altered in function during *Hh* colitis. In steady-state intestine, resident mϕ exhibit an anti-inflammatory phenotype characterised by constitutive production of IL-10 and low levels of TNFα, together with an inability to respond to stimuli such as TLR ligands, but it has been unclear whether these properties can change during inflammation (34). In contrast to their CX3CR1^{hi} counterparts, as we show here, cells within the CX3CR1^{int} compartment are actively pro-inflammatory, expressing much higher levels of mRNA for pro-inflammatory mediators such as IL1β, iNOS, IL-23, and IL-12 during *Hh* colitis than their control counterparts. In parallel, CX3CR1^{hi} mϕ taken at the peak of inflammation showed no increased expression of IL-1β or IL-12 mRNA, and only a modest increase in iNOS and IL-23 mRNA, suggesting some, but limited ability to adopt a pro-inflammatory phenotype under these circumstances. In DSS colitis, we and others have shown that resident mϕ do not acquire pro-inflammatory characteristics (6, 12), but this has been reported in models of colitis where IL-10-mediated signalling is absent, with wider alterations in gene expression than we tested here (18). While this contrasting behaviour in the presence and absence of IL-10 is yet to be confirmed in other models of inflammation, the results are consistent with recent evidence that IL-10 drives permanent, epigenetic silencing of pro-inflammatory genes (35). As a result, the absence of IL-10R-mediated signalling profoundly alters the genetic landscape of

mature intestinal mϕ, allowing them to respond to stimuli to which they are normally resistant (18). Whether IL-10 also controls other aspects of intestinal mϕ differentiation is unclear, although it has been reported that their expression of the scavenger receptor CD163 is dependent on IL-10 (14). Arnold *et al*. showed reduced levels of CD206 on CX3CR1^{hi} mϕ in *Hh* colitis (32), but it is not clear whether this reflects an intrinsic effect of IL-10, or is secondary to the effects of inflammation. That resident mϕ retain a substantial proportion of their homeostatic properties in the absence of IL-10 is suggested by our finding that sustained expansion of this population is not accompanied by maintenance of *Hh*-dependent immunopathology.

The colitis induced by *Hh* is dependent on IL-23 (22) and upregulation of this cytokine was one of the major changes we and others observed in CX3CR1^{int}CD11b^{+} myeloid cells in this model (32). It has often been difficult to identify precisely the cell responsible for producing IL-23 in infection or inflammation, in great part because mϕ and DC share many phenotypic features such as CD11c, MHCII, CX3CR1 and CD11b. Therefore it is important to note that by using rigorous gating strategies based on CD64 as a mϕ marker, both we and Arnold *et al*. (32) show that IL-23 was derived from the mϕ lineage, which is consistent with work in other models (7, 36, 37). Notably, however, we detected increased IL-12p35 and IL-23p19 transcript levels in elicited CX3CR1^{int} monocyte/mϕs, suggesting that these cells produce both IL-12 and IL-23 during *Hh*-induced intestinal inflammation. Thus we propose that the T_H17 response and subsequent phenotype switching of Th17 cells into IFN-γ^{+}IL-17A^{+} lymphocytes in *Hh* colitis (24) is driven by IL-23 derived from mϕ, presumably activated directly by products of the organism. Nevertheless it should be noted that both CD103^{+}CD11b^{+} and CD103^{-}CD11b^{+} DC from the intestine have been shown to be capable of driving T_H17 responses *in vivo* and *in vitro* respectively, via production of IL-23 and/or IL-6

(30, 38-40). Thus there may be flexibility between the mϕ and DC lineages in their ability to stimulate T_H17 activity depending on the stimulus. Alternatively, these cell types may cooperate in driving such T-cell responses, perhaps with migratory DC being responsible for priming T_H17 cells in the draining lymph node, while tissue resident mϕ may sustain the survival of these cells once they migrate back to the mucosa (41).

Together our results show that elicited monocyte-derived $CX3CR1^{int}$ macrophages form the predominant pro-inflammatory macrophage population in *Hh*-induced colitis. Given that these cells appear to derive from the same $Ly6C^{hi}$ blood monocytes as their homeostatic counterparts, identifying the factors that govern monocyte fate in the colon during homeostasis versus inflammation could provide new therapeutic targets for the treatment for IBD.

ACKNOWLEDGEMENTS

This work was supported by the Wellcome Trust (grant number 094763/Z/10/Z; AMM, CCB and MCK). CCB is funded through a Sir Henry Dale Fellowship jointly supported by The Wellcome Trust and The Royal Society (206234/Z/17/Z).

AUTHOR CONTRIBUTIONS

CCB, CJO, CAT, and MCK performed the experiments, analysed the data, and assisted with the manuscript. CCB, MCK, and AMM designed and coordinated the research, interpreted the data, and wrote the manuscript.

REFERENCES

1. **Bain CC**, **Mowat AM**. 2011. Intestinal macrophages - specialised adaptation to a unique environment. Eur J Immunol, 2011 ed. **41**:2494–2498.

2. **Bain CC**, **Mowat AM**. 2014. Macrophages in intestinal homeostasis and inflammation. Immunol Rev **260**:102–117.

3. **Geissmann F**, **Manz MG**, **Jung S**, **Sieweke MH**, **Merad M**, **Ley K**. 2010. Development of monocytes, macrophages, and dendritic cells. Science (New York, NY, 2010 ed. **327**:656–661.

4. **Platt AM**, **Bain CC**, **Bordon Y**, **Sester DP**, **Mowat AM**. 2010. An independent subset of TLR expressing CCR2-dependent macrophages promotes colonic inflammation. J Immunol **184**:6843–6854.

5. **Smythies LE**, **Sellers M**, **Clements RH**, **Mosteller-Barnum M**, **Meng G**, **Benjamin WH**, **Orenstein JM**, **Smith PD**. 2005. Human intestinal macrophages display profound inflammatory anergy despite avid phagocytic and bacteriocidal activity. J Clin Invest, 2005 ed. **115**:66–75.

6. **Bain CC**, **Scott CL**, **Uronen-Hansson H**, **Gudjonsson S**, **Jansson O**, **Grip O**, **Guilliams M**, **Malissen B**, **Agace WW**, **Mowat AM**. 2013. Resident and pro-inflammatory macrophages in the colon represent alternative context-dependent fates of the same Ly6Chi monocyte precursors. Mucosal Immunol, 2012 ed. **6**:498–510.

7. **Kamada N**, **Hisamatsu T**, **Okamoto S**, **Chinen H**, **Kobayashi T**, **Sato T**, **Sakuraba A**, **Kitazume MT**, **Sugita A**, **Koganei K**, **Akagawa KS**, **Hibi T**. 2008. Unique CD14 intestinal macrophages contribute to the pathogenesis of Crohn disease via IL-23/IFN-gamma axis. J Clin Invest, 2008 ed. **118**:2269–2280.

8. **Rugtveit J**, **Nilsen EM**, **Bakka A**, **Carlsen H**, **Brandtzaeg P**, **Scott H**. 1997. Cytokine profiles differ in newly recruited and resident subsets of mucosal macrophages from inflammatory bowel disease. Gastroenterology, 1997 ed. **112**:1493–1505.

9. **Thiesen S**, **Janciauskiene S**, **Uronen-Hansson H**, **Agace W**, **Högerkorp C-M**, **Spee P**, **Häkansson K**, **Grip O**. 2013. CD14hiHLA-DRdim macrophages, with a resemblance to classical blood monocytes, dominate inflamed mucosa in Crohn's disease. Journal of leukocyte biology.

10. **Schridde A**, **Bain CC**, **Mayer JU**, **Montgomery J**, **Pollet E**, **Denecke B**, **Milling SWF**, **Jenkins SJ**, **Dalod M**, **Henri S**, **Malissen B**, **Pabst O**, **Mcl Mowat A**. 2017. Tissue-specific differentiation of colonic macrophages requires TGFβ receptor-mediated signaling. Mucosal Immunol.

11. **Bain CC**, **Bravo-Blas A**, **Scott CL**, **Gomez Perdiguero E**, **Geissmann F**, **Henri S**, **Malissen B**, **Osborne LC**, **Artis D**, **Mowat AM**. 2014. Constant replenishment from circulating monocytes maintains the macrophage pool in the intestine of adult mice. Nature immunology.

12. **Zigmond E**, **Varol C**, **Farache J**, **Elmaliah E**, **Satpathy AT**, **Friedlander G**, **Mack M**, **Shpigel N**, **Boneca IG**, **Murphy KM**, **Shakhar G**, **Halpern Z**, **Jung S**. 2012. Ly6C hi monocytes in the inflamed colon give rise to proinflammatory effector cells and migratory antigen-presenting cells. Immunity, 2012 ed. **37**:1076–1090.

13. **Rivollier A**, **He J**, **Kole A**, **Valatas V**, **Kelsall BL**. 2012. Inflammation switches the differentiation program of Ly6Chi monocytes from antiinflammatory macrophages to inflammatory dendritic cells in the colon. The Journal of experimental medicine, 2012 ed. **209**:139–155.

14. **Hirotani T**, **Lee PY**, **Kuwata H**, **Yamamoto M**, **Matsumoto M**, **Kawase I**, **Akira S**, **Takeda K**. 2005. The nuclear IkappaB protein IkappaBNS selectively inhibits lipopolysaccharide-induced IL-6 production in macrophages of the colonic lamina propria. J Immunol, 2005 ed. **174**:3650–3657.

15. **Takeda K**, **Clausen BE**, **Kaisho T**, **Tsujimura T**, **Terada N**, **Forster I**, **Akira S**. 1999. Enhanced Th1 activity and development of chronic enterocolitis in mice devoid of Stat3 in macrophages and neutrophils. Immunity, 1999 ed. **10**:39–49.

16. **Ueda Y**, **Kayama H**, **Jeon SG**, **Kusu T**, **Isaka Y**, **Rakugi H**, **Yamamoto M**, **Takeda K**. 2010. Commensal microbiota induce LPS hyporesponsiveness in colonic macrophages via the production of IL-10. Int Immunol, 2010 ed. **22**:953–962.

17. **Kuhn R**, **Lohler J**, **Rennick D**, **Rajewsky K**, **Muller W**. 1993. Interleukin-10-deficient mice develop chronic enterocolitis. Cell, 1993rd ed. **75**:263–274.

18. **Zigmond E**, **Bernshtein B**, **Friedlander G**, **Walker CR**, **Yona S**, **Kim K-W**, **Brenner O**, **Krauthgamer R**, **Varol C**, **Muller W**, **Jung S**. 2014. Macrophage-restricted interleukin-10 receptor deficiency, but not IL-10 deficiency, causes severe spontaneous colitis. Immunity **40**:720–733.

19. **Shouval DS**, **Biswas A**, **Goettel JA**, **McCann K**, **Conaway E**, **Redhu NS**, **Mascanfroni ID**, **Adham Al Z**, **Lavoie S**, **Ibourk M**, **Nguyen DD**, **Samsom JN**, **Escher JC**, **Somech R**, **Weiss B**, **Beier R**, **Conklin LS**, **Ebens CL**, **Santos FGMS**, **Ferreira AR**, **Sherlock M**, **Bhan AK**, **Muller W**, **Mora JR**, **Quintana FJ**, **Klein C**, **Muise AM**, **Horwitz BH**, **Snapper SB**. 2014. Interleukin-10 receptor signaling in innate immune cells regulates mucosal immune tolerance and anti-inflammatory macrophage function. Immunity **40**:706–719.

20. **Shouval DS**, **Ouahed J**, **Biswas A**, **Goettel JA**, **Horwitz BH**, **Klein C**, **Muise AM**, **Snapper SB**. 2014. Interleukin 10 receptor signaling: master regulator of intestinal mucosal homeostasis in mice and humans. Adv Immunol **122**:177–210.

21. **Kullberg MC**, **Ward JM**, **Gorelick PL**, **Caspar P**, **Hieny S**, **Cheever A**, **Jankovic D**, **Sher A**. 1998. Helicobacter hepaticus triggers colitis in specific-pathogen-free interleukin-10 (IL-10)-deficient mice through an IL-12- and gamma interferon-dependent mechanism. Infect Immun **66**:5157–5166.

22. **Kullberg MC**, **Jankovic D**, **Feng CG**, **Hue S**, **Gorelick PL**, **McKenzie BS**, **Cua DJ**, **Powrie F**, **Cheever AW**, **Maloy KJ**, **Sher A**. 2006. IL-23 plays a key role in

Helicobacter hepaticus-induced T cell-dependent colitis. The Journal of experimental medicine **203**:2485–2494.

23. **Ward JM**, **Anver MR**, **Haines DC**, **Benveniste RE**. 1994. Chronic active hepatitis in mice caused by Helicobacter hepaticus. Am J Pathol **145**:959–968.

24. **Fox JG**, **Dewhirst FE**, **Tully JG**, **Paster BJ**, **Yan L**, **Taylor NS**, **Collins MJ**, **Gorelick PL**, **Ward JM**. 1994. Helicobacter hepaticus sp. nov., a microaerophilic bacterium isolated from livers and intestinal mucosal scrapings from mice. J Clin Microbiol **32**:1238–1245.

25. **Morrison PJ**, **Bending D**, **Fouser LA**, **Wright JF**, **Stockinger B**, **Cooke A**, **Kullberg MC**. 2013. Th17-cell plasticity in Helicobacter hepaticus-induced intestinal inflammation. Mucosal Immunol **6**:1143–1156.

26. **Bain CC**, **Mowat AM**. 2011. CD200 receptor and macrophage function in the intestine. Immunobiology, 2011 ed.

27. **Kullberg MC**, **Jankovic D**, **Gorelick PL**, **Caspar P**, **Letterio JJ**, **Cheever AW**, **Sher A**. 2002. Bacteria-triggered CD4(+) T regulatory cells suppress Helicobacter hepaticus-induced colitis. The Journal of experimental medicine **196**:505–515.

28. **Tamoutounour S**, **Henri S**, **Lelouard H**, **de Bovis B**, **de Haar C**, **van der Woude CJ**, **Woltman AM**, **Reyal Y**, **Bonnet D**, **Sichien D**, **Bain CC**, **Mowat AM**, **Reis e Sousa C**, **Poulin LF**, **Malissen B**, **Guilliams M**. 2012. CD64 distinguishes macrophages from dendritic cells in the gut and reveals the Th1-inducing role of mesenteric lymph node macrophages during colitis. Eur J Immunol **42**:3150–3166.

29. **Sheng J**, **Ruedl C**, **Karjalainen K**. 2015. Most Tissue-Resident Macrophages Except Microglia Are Derived from Fetal Hematopoietic Stem Cells. Immunity **43**:382–393.

30. **Scott CL**, **Bain CC**, **Wright PB**, **Sichien D**, **Kotarsky K**, **Persson EK**, **Luda K**, **Guilliams M**, **Lambrecht BN**, **Agace WW**, **Milling SW**, **Mowat AM**. 2015. CCR2(+)CD103(-) intestinal dendritic cells develop from DC-committed precursors and induce interleukin-17 production by T cells. Mucosal Immunol **8**:327–339.

31. **Jung S**, **Aliberti J**, **Graemmel P**, **Sunshine MJ**, **Kreutzberg GW**, **Sher A**, **Littman DR**. 2000. Analysis of fractalkine receptor CX(3)CR1 function by targeted deletion and green fluorescent protein reporter gene insertion. Mol Cell Biol, 2000 ed. **20**:4106–4114.

32. **Arnold IC**, **Mathisen S**, **Schulthess J**, **Danne C**, **Hegazy AN**, **Powrie F**. 2015. CD11c(+) monocyte/macrophages promote chronic Helicobacter hepaticus-induced intestinal inflammation through the production of IL-23. Mucosal Immunol.

33. **Hoshi N**, **Schenten D**, **Nish SA**, **Walther Z**, **Gagliani N**, **Flavell RA**, **Reizis B**, **Shen Z**, **Fox JG**, **Iwasaki A**, **Medzhitov R**. 2012. MyD88 signalling in colonic mononuclear phagocytes drives colitis in IL-10-deficient mice. Nat Commun **3**:1120.

34. **Joeris T**, **Müller-Luda K**, **Agace WW**, **Mowat AM**. 2017. Diversity and functions of

intestinal mononuclear phagocytes. Mucosal Immunol.

35. **Simon JM**, **Davis JP**, **Lee SE**, **Schaner MR**, **Gipson GR**, **Weiser M**, **Sartor RB**, **Herfarth HH**, **Rahbar R**, **Sadiq TS**, **Koruda MJ**, **McGovern DP**, **Lieb JD**, **Mohlke KL**, **Furey TS**, **Sheikh SZ**. 2016. Alterations to chromatin in intestinal macrophages link IL-10 deficiency to inappropriate inflammatory responses. Eur J Immunol.

36. **Aychek T**, **Mildner A**, **Yona S**, **Kim K-W**, **Lampl N**, **Reich-Zeliger S**, **Boon L**, **Yogev N**, **Waisman A**, **Cua DJ**, **Jung S**. 2015. IL-23-mediated mononuclear phagocyte crosstalk protects mice from Citrobacter rodentium-induced colon immunopathology. Nat Commun **6**:6525.

37. **Panea C**, **Farkas AM**, **Goto Y**, **Abdollahi-Roodsaz S**, **Lee C**, **Koscsó B**, **Gowda K**, **Hohl TM**, **Bogunovic M**, **Ivanov II**. 2015. Intestinal Monocyte-Derived Macrophages Control Commensal-Specific Th17 Responses. Cell Rep **12**:1314–1324.

38. **Persson EK**, **Uronen-Hansson H**, **Semmrich M**, **Rivollier A**, **Hägerbrand K**, **Marsal J**, **Gudjonsson S**, **Håkansson U**, **Reizis B**, **Kotarsky K**, **Agace WW**. 2013. IRF4 transcription-factor-dependent CD103(+)CD11b(+) dendritic cells drive mucosal T helper 17 cell differentiation. Immunity **38**:958–969.

39. **Schlitzer A**, **McGovern N**, **Teo P**, **Zelante T**, **Atarashi K**, **Low D**, **Ho AW**, **See P**, **Shin A**, **Wasan PS**, **Hoeffel G**, **Malleret B**, **Heiseke A**, **Chew S**, **Jardine L**, **Purvis HA**, **Hilkens CM**, **Tam J**, **Poidinger M**, **Stanley ER**, **Krug AB**, **Renia L**, **Sivasankar B**, **Ng LG**, **Collin M**, **Ricciardi-Castagnoli P**, **Honda K**, **Haniffa M**, **Ginhoux F**. 2013. IRF4 transcription factor-dependent CD11b+ dendritic cells in human and mouse control mucosal IL-17 cytokine responses. Immunity, 2013 ed. **38**:970–983.

40. **Satpathy AT**, **Briseño CG**, **Lee JS**, **Ng D**, **Manieri NA**, **Kc W**, **Wu X**, **Thomas SR**, **Lee W-L**, **Turkoz M**, **McDonald KG**, **Meredith MM**, **Song C**, **Guidos CJ**, **Newberry RD**, **Ouyang W**, **Murphy TL**, **Stappenbeck TS**, **Gommerman JL**, **Nussenzweig MC**, **Colonna M**, **Kopan R**, **Murphy KM**. 2013. Notch2-dependent classical dendritic cells orchestrate intestinal immunity to attaching-and-effacing bacterial pathogens. Nature immunology **14**:937–948.

41. **Shaw MH**, **Kamada N**, **Kim Y-G**, **Núñez G**. 2012. Microbiota-induced IL-1β, but not IL-6, is critical for the development of steady-state TH17 cells in the intestine. The Journal of experimental medicine **209**:251–258.

553

554 **FIGURE LEGENDS**

555 **Figure 1. Expansion of myeloid cells in the large intestine of *Hh-infected* colitic *Il10*$^{-/-}$**
556 **mice.** WT and *Il10*$^{-/-}$ mice were inoculated with *Hh*, and LP cells were isolated from pooled
557 caecum and colon 2 weeks (**A-B**) or 1, 3, 5, 8, and 11 days (**C**) later and examined by flow
558 cytometry. Uninfected mice were included as controls. (**A**) Total numbers of LP cells (left
559 panel), percentage (middle panel) and total numbers (right panel) of CD45$^+$ hematopoietic
560 cells from uninfected (white bars) and 2-week *Hh*-infected (black bars) WT and *Il10*$^{-/-}$ mice.
561 (**B**) Numbers of B220$^+$CD19$^+$ B cells (left panel), CD3$^+$CD4$^+$ T cells (middle panel), and
562 CD11b$^+$ myeloid cells (right panel) from uninfected (white bars) and 2-week *Hh-infected*
563 (black bars) WT and *Il10*$^{-/-}$ mice. Data in **A**-**B** are from one representative experiment out of
564 at least three performed, and bars represent mean + SD of 3 mice per group. (**C**) Total
565 numbers of LP cells (left panel), CD45$^+$ hematopoietic cells (middle panel) and CD11b$^+$ cells
566 (right panel) from pooled caecum and colon of 1-, 3-, 5-, 8-, and 11-day *Hh*-infected *Il10*$^{-/-}$
567 mice. Data are pooled from two individual experiments, and are the mean + SD of 5-6 LP cell
568 preparations (each pooled from 1-2 animals) from *Hh*-infected mice and 8 cell preparations
569 (each pooled from 2-3 animals) from uninfected mice. One-way ANOVA followed by Tukey's
570 multiple comparison test. ***P<0.001, ****P<0.0001 when comparing *Hh*-infected and
571 uninfected mice (A-B) or when compared to uninfected mice (C).

572

573 **Figure 2. Large intestinal CD11b$^+$ myeloid cells from *Hh-infected Il10*$^{-/-}$ mice secrete**
574 **elevated amounts of pro-inflammatory cytokines following TLR stimulation.** *Il10*$^{-/-}$ mice
575 were inoculated with *Hh*, and LP cells were isolated from pooled caecum and colon 2 weeks
576 later. Uninfected mice were included as controls. (**A-B**) Large intestinal LP cells were cultured

in medium alone or stimulated with 10 μg/ml Pam3CSK4 for 4 hours with 10 μg/ml brefeldin A during the last 3 hours, and then stained for CD45, CD11b, and TNFα or appropriate isotype control. Dot plots in **A** are gated on $CD45^+CD11b^+$ LP cells from uninfected (Uninf.; upper panels) and 2-week *Hh*-infected *Il10*$^{-/-}$ mice (lower panels), and numbers (+ SD) of $TNF\alpha^+$ $CD11b^+$ cells per mouse in **B** were calculated from the percentages in A and the total number of cells isolated from each mouse. Data in **A-B** are representative of two independent experiments performed with 3 individual mice per group. One-way ANOVA followed by Tukey's multiple comparison test. **P<0.01 and ****P<0.0001. (**C**) Large intestinal LP $CD11b^+$ myeloid cells were FACS-purified from uninfected (white bars) and 2-week *Hh*-infected (black bars) *Il10*$^{-/-}$ mice and stimulated *in vitro* with LPS (10 μg/ml), Pam3CSK4 (10 μg/ml), or SHelAg (10 μg/ml) or cultured in medium alone. After 24 hours, supernatants were collected and analyzed for the presence of IL-12p40, IL-6, and TNFα. Bars represent mean + SD of quadruplicate (IL-12p40 and IL-6) or duplicate (TNFa) ELISA values (where each value represents a separate culture) combined from two independent experiments. (**D**) RT-qPCR analysis of IL-12p35 (*Il12a*), IL-12p40 (*Il12b*), and IL-23p19 (*Il23a*) transcripts relative to HPRT in sorted $CD11b^+$ cells from uninfected (white bars) or 2-week *Hh*-infected (black bars) *Il10*$^{-/-}$ mice. Bars represent means + SD of three (for uninfected mice) and four (for *Hh*-infected mice) individual experiments, each consisting of cells pooled from 5-6 mice. Mann Whitney test. *P<0.05.

Figure 3. Composition of the myeloid compartment in *Hh*-infected *Il10*$^{-/-}$ mice. WT and *Il10*$^{-/-}$ mice were inoculated with *Hh* and colonic LP cells were isolated 2 weeks later and examined by flow cytometry. Uninfected mice were included as controls. (**A**) Relative frequencies amongst total colonic $CD11b^+$ cells of $Ly6G^+$ neutrophils, SSC^{hi} $MHCII^-$

eosinophils, CD64$^-$ CD11c$^+$ MHCII$^+$ CD11b$^+$ DC and Ly6C/MHCII-defined cells of the CD64$^+$ monocyte/macrophage compartment (Ly6C^{hi}MHCII$^-$, Ly6C$^+$MHCII$^+$, Ly6C$^-$MHCII$^+$) from uninfected or *Hh*-infected WT and *Il10*$^{-/-}$ mice. (**B-C**) Absolute numbers of Ly6G$^+$ neutrophils (**B**) and SSC^{hi} MHCII$^-$ eosinophils (**C**) per colon of uninfected or *Hh*-infected WT and *Il10*$^{-/-}$ mice. (**D**) Representative expression of Ly6C and MHCII by CD11b$^+$Ly6G$^-$SSC^{lo}CD64$^+$ cells from uninfected or *Hh*-infected WT and *Il10*$^{-/-}$ mice. Bar graph shows the frequency amongst CD11b$^+$Ly6G$^-$SSC^{lo}CD64$^+$ cells of Ly6C^{hi}MHCII$^-$, Ly6C$^+$MHCII$^+$ and Ly6C$^-$MHCII$^+$ cells. (**E**) Absolute numbers of Ly6C^{hi}MHCII$^-$, Ly6C$^+$MHCII$^+$ and Ly6C$^-$MHCII$^+$ cells per colon of uninfected or *Hh*-infected WT and *Il10*$^{-/-}$ mice. Data are from one of two independent experiments performed. Bars represent the mean + SD of 4 individual mice per group. One-way ANOVA followed by Tukey's multiple comparison test. ****P<0.0001

Figure 4. Monocyte differentiation is dysregulated in anti-IL-10R-treated *Hh*-infected colitic *Cx3cr1*$^{+/gfp}$ mice. *Cx3cr1*$^{+/gfp}$ mice were inoculated with *Hh* and treated weekly with anti-IL-10R to induce colitis. The composition of the colonic myeloid compartment was then examined at 14, 41 and 77 days post infection and compared to uninfected mice or mice given *Hh* alone. (**A-B**) Absolute numbers of total CD45$^+$ (**A**) and CD11b$^+$ cells (**B**) per colon of *Hh*/anti-IL-10R-treated mice 14, 41 and 77 days after infection, compared with control mice (uninfected and *Hh* alone; data pooled from day 14-77 for these groups). (**C**) Relative frequencies amongst total colonic CD11b$^+$ cells of Ly6G$^+$ neutrophils, SSC^{hi}MHCII$^-$ eosinophils, F4/80$^-$CD11c$^+$MHCII$^+$CD11b$^+$ DC and Ly6C/MHCII-defined cells of the F4/80$^+$ monocyte/mϕ compartment (Ly6C^{hi}MHCII$^-$, Ly6C$^+$MHCII$^+$, Ly6C$^-$MHCII$^+$) of mice as in **A**. (**D-E**) Representative expression of Ly6C and MHCII by CD11b$^+$Ly6G$^-$SSC^{lo}F4/80$^+$ cells (**D**) and absolute numbers of Ly6C^{hi}MHCII$^-$, Ly6C$^+$MHCII$^+$ and Ly6C$^-$MHCII$^+$ cells per colon (**E**) of

mice as in **A**. (**F**) Representative expression of CX3CR1-GFP by Ly6C$^-$MHCII$^+$ cells from uninfected mice, mice inoculated with *Hh* alone, and mice receiving *Hh* plus anti-IL-10R when analysed at 14, 41 and 77 post inoculation. The histograms for the uninfected and *Hh* alone are taken from the day 14 experiment. (**G**) Absolute numbers of CX3CR1^{int} (top panel) and CX3CR1^{hi} (bottom panel) Ly6C$^-$ MHCII$^+$ cells per colon of mice as in **A**. Data are from one experiment and bars represent the mean + SD of 4 individual mice per group. One-way ANOVA followed by Tukey's multiple comparison test. *P<0.05, **P<0.01, ***P<0.001.

Figure 5. Colonic CX3CR1^{int} monocytes/mϕs produce pro-inflammatory mediators during *Hh* colitis. *Cx3cr1*$^{+/gfp}$ mice were inoculated with *Hh* and treated weekly with anti-IL-10R to induce colitis. Two weeks later colonic LP CD64$^+$CX3CR1^{int} and CD64$^+$CX3CR1^{hi} cells (both pre-gated on CD45$^+$CD11b$^+$Ly6G$^-$SiglecF$^-$) were FACS-purified and processed for RT-qPCR analysis of pro-inflammatory mediators. Uninfected mice, mice given *Hh* alone, and mice given anti-IL-10R alone were included as controls. Transcript levels of IL-1β (*Il1b*) (**A**), iNOS (*Nos2*) (**B**), IL-23 (*Il23a*) (**C**) and IL-12p35 (*Il12a*) (**D**) relative to TATA-binding protein (TBP) in uninfected, *Hh* alone, anti-IL-10R alone, and *Hh* plus anti-IL-10R groups. Each symbol represents a pool of 3 mice (for uninfected, *Hh* alone, and anti-IL-10R alone) or individual mice (for *Hh* plus anti-IL-10R). Data are pooled from two individual experiments. Unpaired Student's t test. *P<0.05, **P<0.01, ***P<0.001.

Figure 1

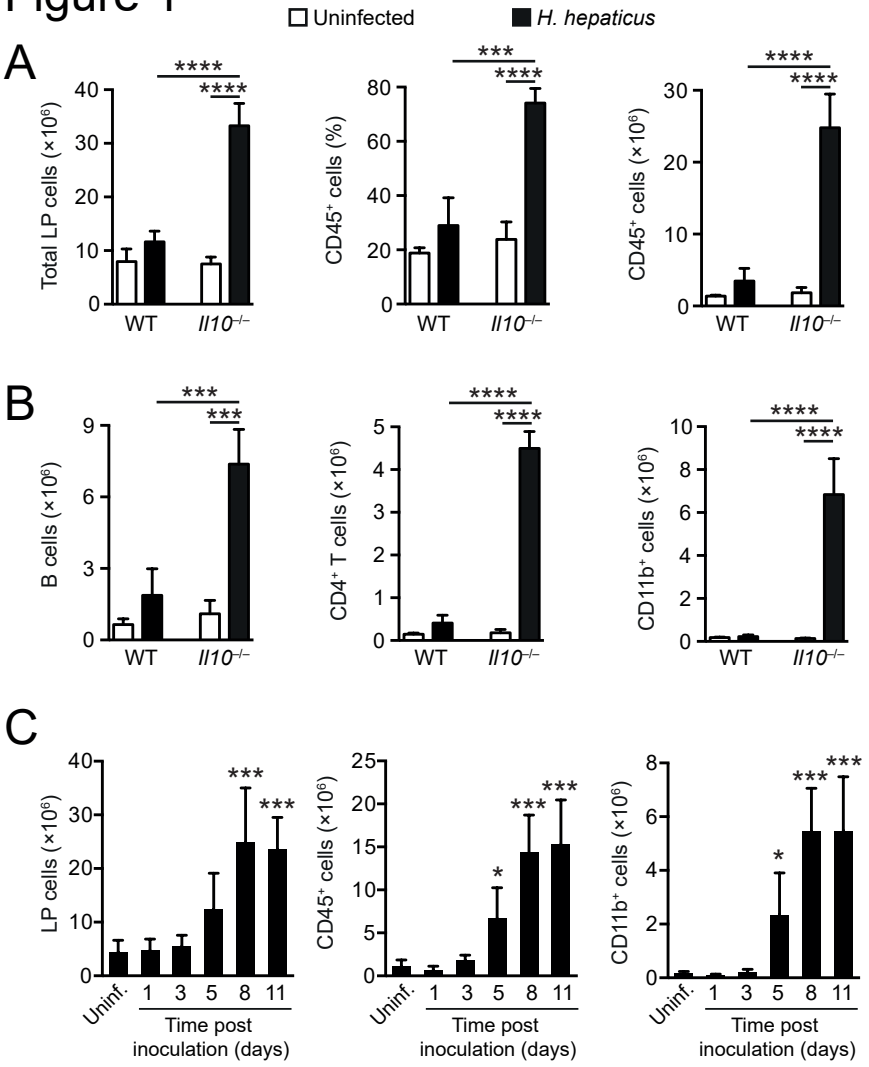

Figure 2

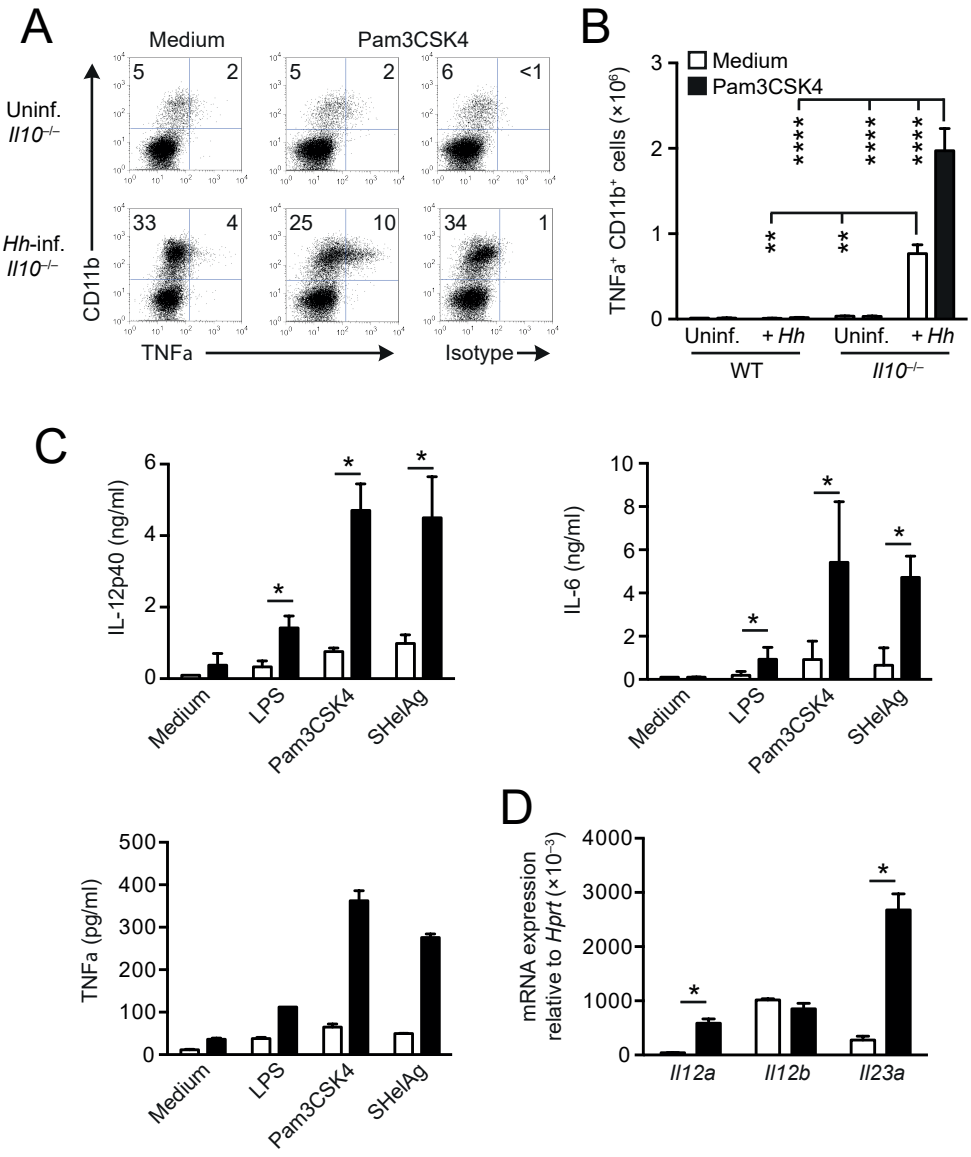

Figure 3

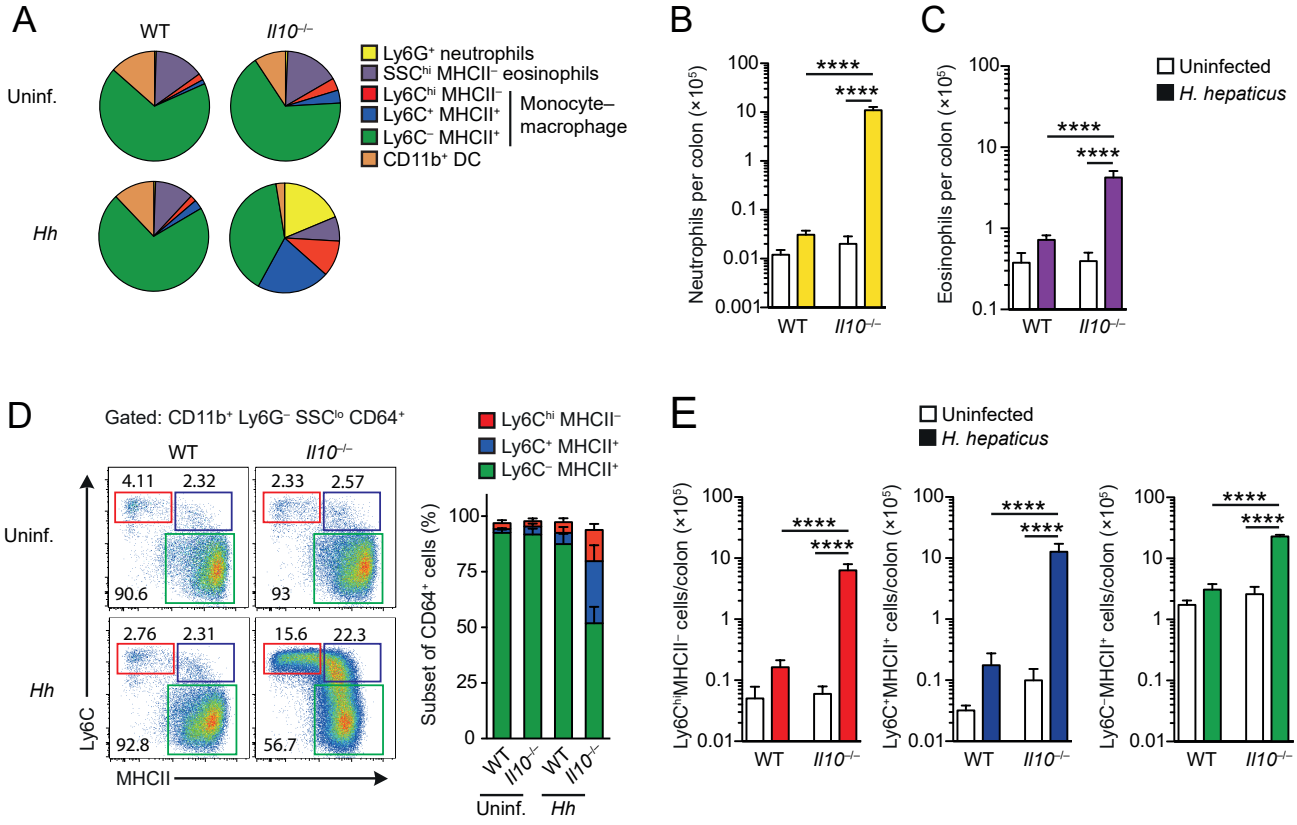

Figure 4

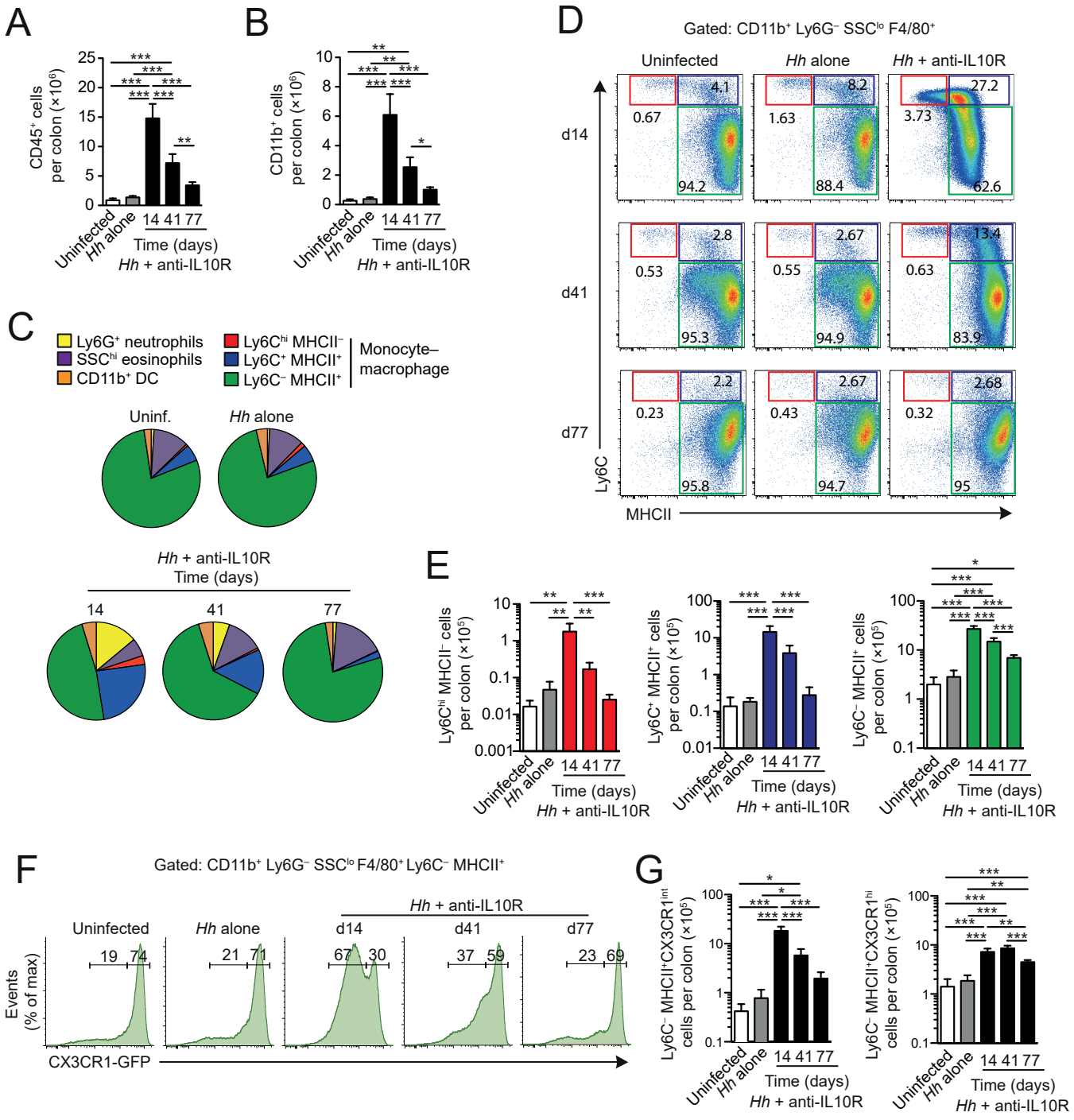

Figure 5